Axl Promotes Cutaneous Squamous Cell Carcinoma Survival through Negative Regulation of Pro-Apoptotic Bcl-2 Family Members

Emmanouil S. Papadakis[1], Monika A. Cichoń[1], Jashmin J. Vyas[1], Nakul Patel[1], Lucy Ghali[2], Rino Cerio[1], Alan Storey[3] and Edel A. O'Toole[1]

Expression of Axl, a receptor tyrosine kinase, is increased in cutaneous squamous cell carcinoma (SCC). Examination of a series of cutaneous SCC tumors revealed positive phospho-Akt (P-Akt) staining accompanied by weak TUNEL staining in Axl-positive tumors, suggesting an anti-apoptotic role for Axl in SCC survival. The role of Axl in UV-induced apoptosis was investigated in a cutaneous SCC cell line using retroviral short hairpin RNA sequences enabling stable Axl knock-down. We show that, although Axl knock-down has no effect on cell proliferation, it sensitizes cells to UV-induced apoptosis through increased activation of the pro-apoptotic protein Bad, a change in the conformation of Bax and Bak, release of cytochrome *c* into the cytosol, and activation of caspases. These events are accompanied by faster Akt dephosphorylation in UV-treated Axl knock-down cells and correlate with the degree of Axl knock-down. Treatment with the pan-caspase inhibitor zVAD-fmk partially rescued cells from UV-induced apoptosis but did not affect Bid cleavage or cytochrome *c* release, suggesting that cells die via the mitochondrial-mediated pathway. Thus, Axl confers resistance of SCC cells to apoptosis and displays potential as a target for therapeutic intervention in cutaneous SCC.

Journal of Investigative Dermatology (2011) **131,** 509–517; doi:10.1038/jid.2010.326; published online 11 November 2010

INTRODUCTION

Squamous cell carcinoma (SCC) accounts for approximately 20% of all cutaneous malignancies and occurs on UV-exposed body sites (Diepgen and Mahler, 2002). About 4% of cutaneous SCCs metastasize (Brantsch *et al.*, 2008) and these patients have a 5-year survival of 25%, highlighting the need to improve therapy.

We recently reported that expression of the receptor tyrosine kinase, Axl, is upregulated in SCC skin tumors *in vivo* (Green *et al.*, 2006). Overexpression of Axl has been associated with invasion and metastasis in various cancers (Meric *et al.*, 2002; Sainaghi *et al.*, 2005; Lay *et al.*, 2007; Sawabu *et al.*, 2007). Axl, in conjunction with its ligand, growth arrest-specific gene 6 (Gas6), can enhance cell survival. Recent data have shown that Axl signaling can prolong malignant glioma growth in mouse brain (Vajkoczy *et al.*, 2006).

Following a cell death signal, a number of apoptotic factors, including cytochrome *c*, are released from the mitochondrial intermembrane space into the cytosol, by a mechanism that allows selective permeabilization of the outer mitochondrial membrane (OMM) (Kluck *et al.*, 1997). The anti-apoptotic proteins, Bcl-2, Bcl-X_L, and Mcl-1, antagonize the release of cytochrome *c* from the mitochondria and subsequent caspase activation, whereas the pro-apoptotic proteins, Bax and Bak, promote apoptosis (Wei *et al.*, 2001). Inhibitory molecules, such as Bad, bind to anti-apoptotic Bcl-2/Bcl-X_L proteins, thereby preventing their sequestration of molecules such as cleaved Bid (tBid) or Bim that can directly activate Bax and Bak (Letai *et al.*, 2002; Kuwana and Newmeyer, 2003; Kim *et al.*, 2006).

Immunohistochemical analysis revealed increased phospho-Akt (P-Akt) staining with significantly lower TUNEL staining in Axl-positive tumors and led us to examine the mechanisms by which Axl regulates apoptosis in cutaneous SCC cells. Retroviral gene delivery of Axl-targeting short hairpin RNA (shRNA) sequences was used to achieve stable Axl knock-down. Our results demonstrate that Axl contributes to the malignant SCC phenotype by protecting cells from UV-induced apoptosis through modulation of the Akt and associated PTEN pathways and suppression of the pro-apoptotic activity of Bcl-2 family members.

[1]*Centre for Cutaneous Research, Blizard Institute of Cell and Molecular Science, Barts and the London School of Medicine and Dentistry, Queen Mary University of London, London, UK;* [2]*Department of Natural Sciences, Middlesex University, Enfield, UK and* [3]*Department of Molecular Oncology, The Weatherall Institute of Molecular Medicine, John Radcliffe Hospital, Oxford, UK*

Correspondence: Edel A. O'Toole, Centre for Cutaneous Research, Blizard Institute of Cell and Molecular Science, Barts and the London School of Medicine and Dentistry, Queen Mary University of London, 4 Newark Street, London E1 2AT, UK. E-mail: e.a.otoole@qmul.ac.uk

Received 9 December 2009; revised 18 August 2010; accepted 9 September 2010; published online 11 November 2010

RESULTS

Negative correlation between Axl protein expression and apoptosis in cutaneous SCC tumors

As Axl has been reported to signal via Akt in various cancers, thereby protecting them from apoptosis, we hypothesized that there may be a correlation between Axl, P-Akt, and apoptosis in cutaneous SCC tumors. Sections from 15 SCCs were scored for staining intensity between 0 (no staining) and 3 (intense staining). In contrast to normal skin, which expresses minimal P-Akt, 11/15 (73%) SCCs exhibited P-Akt staining. Axl staining was detected in 10/15 (67%) SCCs, whereas 6/15 (40%) SCCs showed apoptotic cells detected by TUNEL staining. Staining for P-Akt was strong in Axl-positive tumors and was accompanied by significantly decreased TUNEL staining, whereas Axl-negative tumors exhibited weak P-Akt and strong TUNEL staining (Figure 1a). Samples were subdivided into positive (2–3) and weak or negative (0–1) Axl staining for analysis. Median values (bars ± SD) on the graph correspond to P-Akt or TUNEL staining in the Axl-positive and -negative tumors (Figure 1b). There was no correlation between Axl expression and differentiation status.

Knock-down of Axl sensitizes MET1 SCC cells to UV-induced apoptosis

In order to investigate the role of Axl in apoptosis, sustained Axl knock-down was achieved in MET1 SCC cells using shRNA sequences 1053 and 2833. Immunoblotting of total cell lysates from 1053- and 2833-transduced cells revealed a 49% and 92% mean Axl knock-down, respectively (Figure 2a), without any effect on cell proliferation (Figure 2b). Mitochondrial apoptosis involves activation of caspase 3, which is responsible for proteolytic cleavage of the nuclear enzyme poly(ADP-ribose) polymerase (PARP) to bring about cell disassembly (Kaufmann *et al.*, 1993). Immunoblotting showed that treatment with UV up to 24 hours resulted in a small fluctuation of Axl expression levels (Figure 2c), which varied between replicate experiments. Moreover, we observed greater cleavage of caspase 3 and PARP in Axl knock-down compared with pSUPERIOR.retro.puro vector (pSup) cells (Figure 2c). Findings were replicated in a second cell line, SCC-IC 1 (see Supplementary Figure S1 online). Apoptosis increased over time, so that 24 hours after UV treatment there were 17% pSup, 27% 1053, and 50% 2833 apoptotic cells (Figure 2d). Thus, abrogation of Axl expression leads to increased sensitivity to UV-induced apoptosis, correlating with the degree of Axl knock-down.

Knock-down of Axl increases basal phosphorylation of PTEN and the pro-apoptotic potential of Bad

We next investigated the effect of Axl knock-down on Akt and associated pathways in SCC cells. Immunoblotting showed a pronounced time-dependent decrease in Akt phosphorylation in response to UV treatment, which was proportional to the degree of Axl knock-down, whereas total Akt levels remained unchanged (Figure 3a). A downstream Akt target that has a critical role in mediating apoptosis is the pro-apoptotic protein Bad (Zha *et al.*, 1996; Datta *et al.*, 1997). Total levels of Bad expression remained largely unchanged by UV treatment, whereas there was a greater decline in the phosphorylation of Bad in 2833 MET1 cells (Figure 3a). Dephosphorylation of PTEN, a key tumor suppressor, at the C-terminal tail, decreases its stability while enhancing its function as an antagonist of PI3K/Akt signaling (Stambolic *et al.*, 1998; Vazquez *et al.*, 2000). Immunoblotting revealed that knock-down of Axl enhanced basal phosphorylation of phospho-PTEN. In addition, a greater decrease in the total expression levels of PTEN was observed over the time course of UV treatment in Axl knock-down cells (Figure 3a). In order to verify the role of Akt in modulating resistance to apoptosis, MET1 cells were pre-treated with SH5, a selective inhibitor of Akt activity (Figure 3b). This

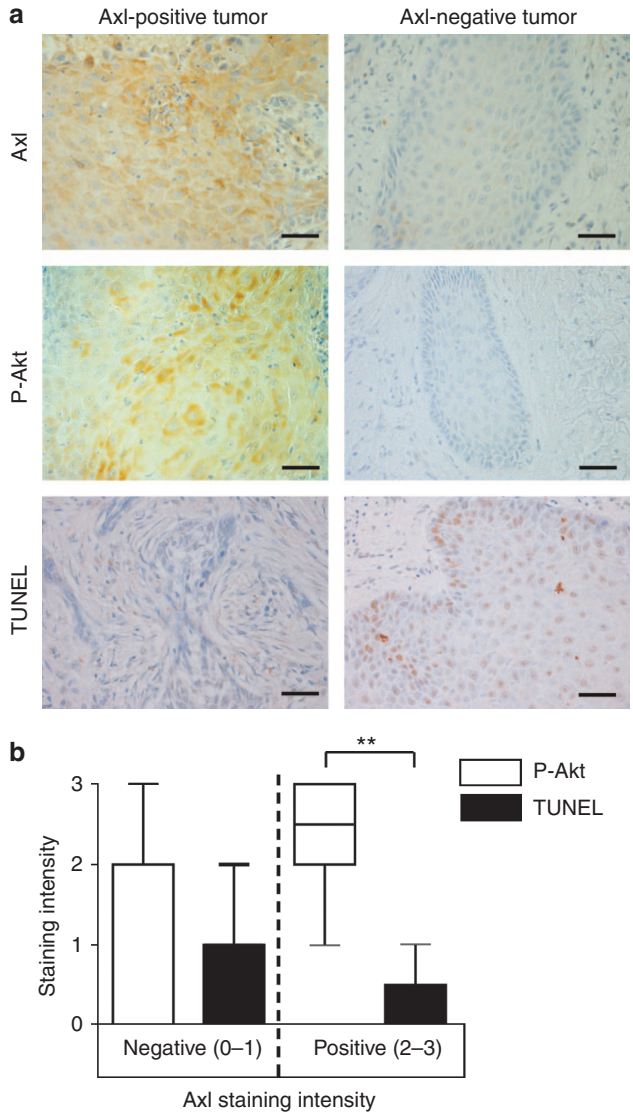

Figure 1. Correlation between Axl, P-Akt, and TUNEL staining in a series of SCC tumors. (**a**) Staining for P-Akt and TUNEL in Axl-positive and -negative SCC tumors. (**b**) Around 15 tumors were stained for Axl, P-Akt, and TUNEL. The intensity of staining was scored from 0 (no staining) to 3 (intense staining). Samples were subdivided into positive (2–3) and weak or negative (0–1) Axl staining. Median values (bars ± SD) on the graph correspond to P-Akt or TUNEL staining in the positive and negative cells. $^{**}P<0.01$. Bar = 100 μm.

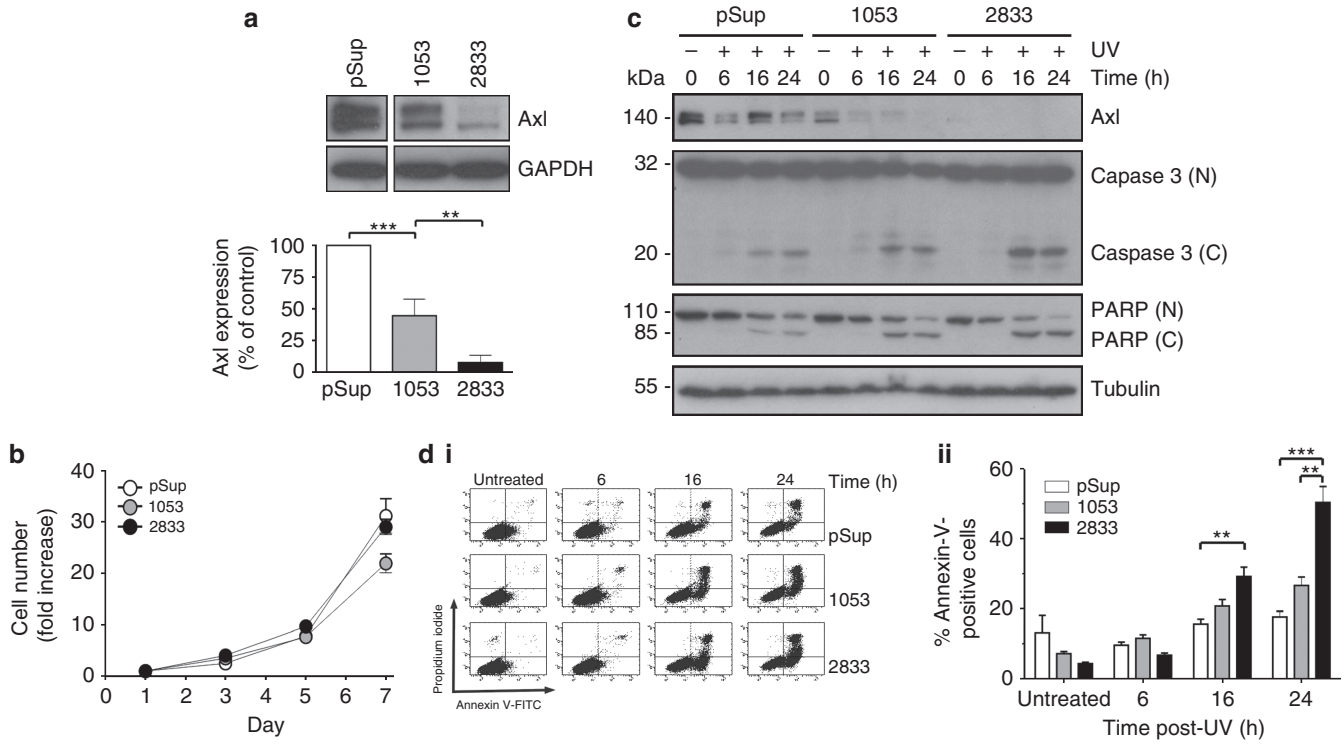

Figure 2. Axl knock-down renders MET1 cells susceptible to apoptosis. (**a**) Axl expression was analyzed by immunoblot of cell lysates from MET1 cells transduced with pSup vector alone or Axl-targeting shRNA sequences 1053 or 2833 (irrelevant lanes between pSup and 1053 were removed). (**b**) Cell proliferation was assessed by counting cells using trypan blue exclusion at the indicated times. Data shown are from three independent experiments. (**c**) pSup, 1053, and 2833 cells were exposed to UV (20 mJ cm^{-2}) and expression levels of Axl, caspase 3, and PARP were detected in cell lysates by immunoblotting. Tubulin was used as a loading control. The data are representative of three independent experiments. (**d**) Apoptosis was quantified by Annexin V-FITC/PI staining of pSup, 1053, and 2833 cells treated with UV for the indicated times. (i) Scatter plots from one experiment are shown; (ii) data (mean ± SEM) from two experiments expressed as % Annexin-V-positive cells are shown. C, cleaved; N, native. $^{**}P<0.01$, $^{***}P<0.001$.

resulted in a significant increase in apoptosis 16 hours after treatment with UV, which correlated with the degree of Axl knock-down, suggesting that Axl functions via Akt to protect SCC cells from apoptosis (Figure 3c).

Knock-down of Axl enhanced UV-induced activation of Bax and Bak in MET1 cells

The pro-apoptotic proteins Bax and Bak regulate mitochondrial cytochrome *c* release through the formation of pores in the OMM (Wei *et al.*, 2001), while Bcl-2, Bcl-X_L, and Mcl-1 are antagonists of Bax and Bak activation (Kim *et al.*, 2006). Immunoblotting showed no change in Bcl-2 or Bcl-X_L expression and Mcl-1 was degraded equally in response to UV treatment in both Axl knock-down and pSup cells (Figure 4a), indicating its dissociation from Bak, which is known to trigger apoptosis (Nijhawan *et al.*, 2003). Although expression levels of Bak remained relatively unaltered, there was an increase in the expression of Bax over the time course of UV treatment (Figure 4a). Activation of Bax and Bak was examined by conformation-specific monoclonal antibodies. Axl knock-down cells exhibited greater Bak and Bax activities compared with pSup cells, proportional to the degree of Axl knock-down, in response to UV with maximal activation at 16 hours (Figure 4b and c). We next examined the translocation of active monomeric Bax from the cytosol to the mitochondria by confocal microscopy. Results showed that movement of Bax to the mitochondria (yellow staining) occurred within 6 hours of UV treatment and was greater in 2833 compared with pSup cells (Figure 4d). These data show that knock-down of Axl in MET1 SCC cells results in a change in the conformation of Bak and Bax in response to UV treatment.

Increased cytochrome *c* release in the cytosol of UV-treated Axl knock-down cells

To measure mitochondrial membrane potential ($\Delta\psi m$), cells were stained with the potential-sensitive dye tetramethylrhodamine ethyl ester perchlorate (TMRE) and 4,6-diamidino-2-phenylidole (DAPI) before FACS processing; DAPI-positive cells were gated out for the analysis. Treatments with $NaNO_3$ or CCCP were used as positive controls. An almost equal drop in $\Delta\psi m$ of approximately 30% was observed as early as 16 hours after UV treatment in all cells (Figure 5a). To examine cytochrome *c* release into the cytosol, cells were permeabilized with a hypertonic digitonin-containing solution. Immunoblotting exhibited a greater cytochrome *c* release in the cytosol of Axl knock-down compared with pSup cells (Figure 5b). These results show that although knock-down of Axl does not seem to affect $\Delta\psi m$, it results in cytochrome *c* release into the cytosol in a regulated way.

Axl knock-down enhances caspase activation and leads to caspase-dependent apoptosis

To further determine the role of Axl in apoptosis following cytochrome *c* release, the activities of caspases 3 and 8 were measured in response to UV. Data revealed that caspase 3 activity in pSup, 1053, and 2833 cells increased by 4.0-, 6.5-, and 8.0-fold, respectively, after 24 hours of UV treatment (Figure 6a). Similarly, caspase 8 activity increased by 2.5-, 4.0-, and 5.6-fold in pSup, 1053, and 2833, respectively (Figure 6b). Activity of both was completely blocked when cells were treated with UV for 24 hours in the presence of the pan-caspase inhibitor zVAD-fmk (Figure 6a and b). These results indicate that UV-induced caspase activation increases with the degree of Axl knock-down. Next, MET1 cells were treated with UV in the presence of zVAD-fmk and apoptotic cells were quantified by Annexin V-FITC/PI staining. Our data show that UV-induced cell death is partly caspase dependent (Figure 6c).

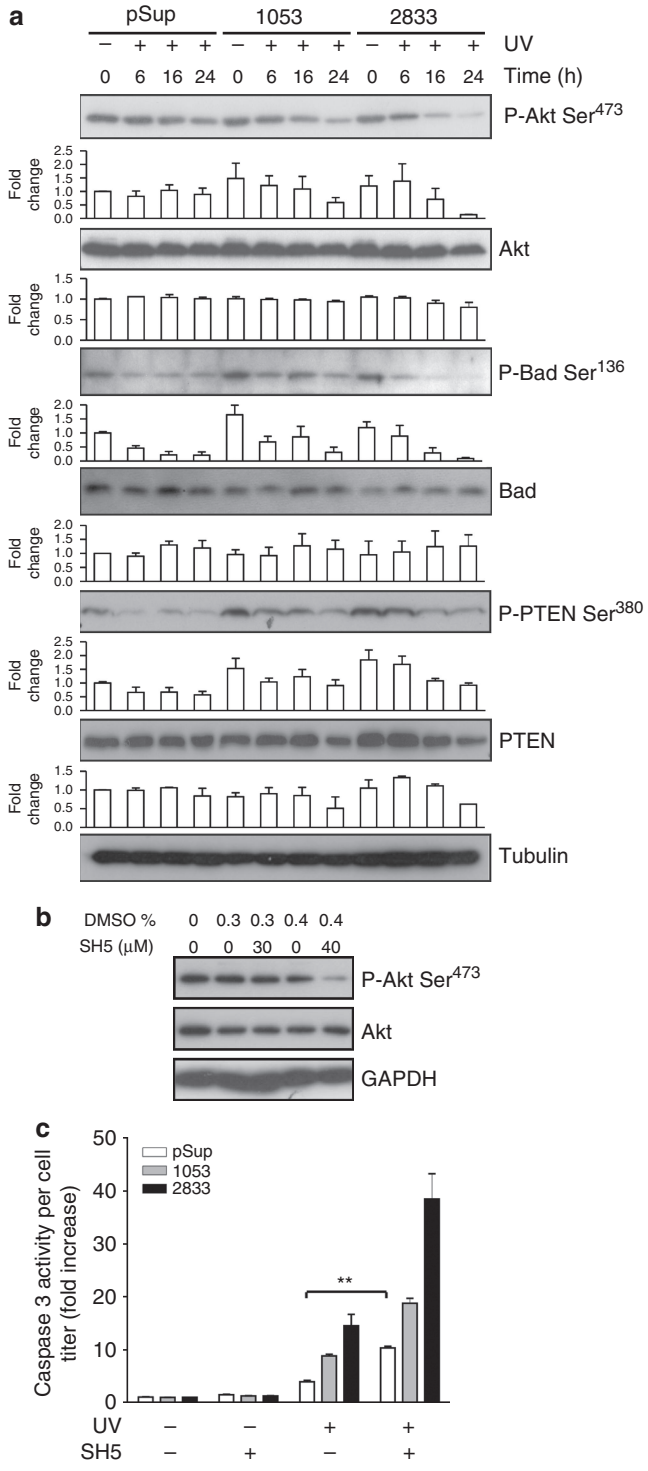

Knock-down of Axl affects expression levels of Bid

Bid is a key pro-apoptotic BH3-only molecule linking the receptor- and mitochondria-mediated apoptotic pathways. Cleavage and activation of native p22 Bid by caspase 8 results in the generation of p15 tBid, which has a role in the activation of Bax and Bak and cytochrome *c* release (Luo *et al.*, 1998). Immunoblotting of total cell lysates revealed a striking decrease in the basal expression levels of Bid, which was proportionate to the degree of Axl inhibition in MET1 cells (Figure 6d). However, levels of tBid were similar in Axl knock-down and pSup cells 24 hours after treatment with UV (Figure 6d). Thus, although Axl seems to have a role in modulating Bid expression, it does not seem to affect Bid processing. As an increase in caspase 8 activity was observed in response to UV treatment in MET1 cells (Figure 6b), we wanted to clarify the role of Bid in UV-induced death in SCC cells. Immunoblot analysis revealed that although treatment with zVAD-fmk inhibited proteolytic processing of Bid, it did not affect the amount of cytochrome *c* released in response to UV (Figure 6e). Inhibition of Bid expression using transient small interfering RNA (siRNA) transfection (Figure 6f) exhibited no significant change in UV-induced apoptosis (Figure 6f). These data indicate that cytochrome *c* release occurs upstream of caspase activation, whereas proteolytic processing of Bid appears to be a downstream event.

DISCUSSION

A major feature of SCC cells is their resistance to apoptosis (Erb *et al.*, 2005). Immunohistochemical analysis of SCC tumors revealed a correlation between Axl and P-Akt staining with a reduction in TUNEL staining in Axl-positive tumors, leading us to investigate further the mechanism by which Axl promotes tumor cell survival. Knock-down of Axl in MET1

Figure 3. Effect of Axl knock-down on the activation of Akt, Bad, and PTEN in response to UV. (**a**) pSup, 1053, and 2833 MET1 cells were exposed to UV (20 mJ cm^{-2}) for the indicated times and expression levels of Akt, P-Akt Ser^{473}, Bad, P-Bad Ser^{136}, PTEN, and P-PTEN Ser^{380} were detected in total cell lysates by immunoblotting. Tubulin was used as a loading control. Bar graphs show the fold change (mean ± SD) in protein expression from two to three blots. (**b**) Immunoblot analysis showing expression levels of Akt and P-Akt Ser^{473} after a dose–response treatment using the specific inhibitor of Akt activity SH5. DMSO was used as a vehicle control, while GAPDH was used as a loading control. (**c**) pSup, 1053, and 2833 MET1 cells were pre-treated with SH5 (40 μM) for 1 hour and were subsequently treated with UV (20 mJ cm^{-2}) for 16 hours. Apoptosis was determined by calculating the ratio of caspase 3 activity over cellular ATP content (cell titer). Data (mean ± SEM) are expressed as fold change of respective controls. $^{**}P<0.01$.

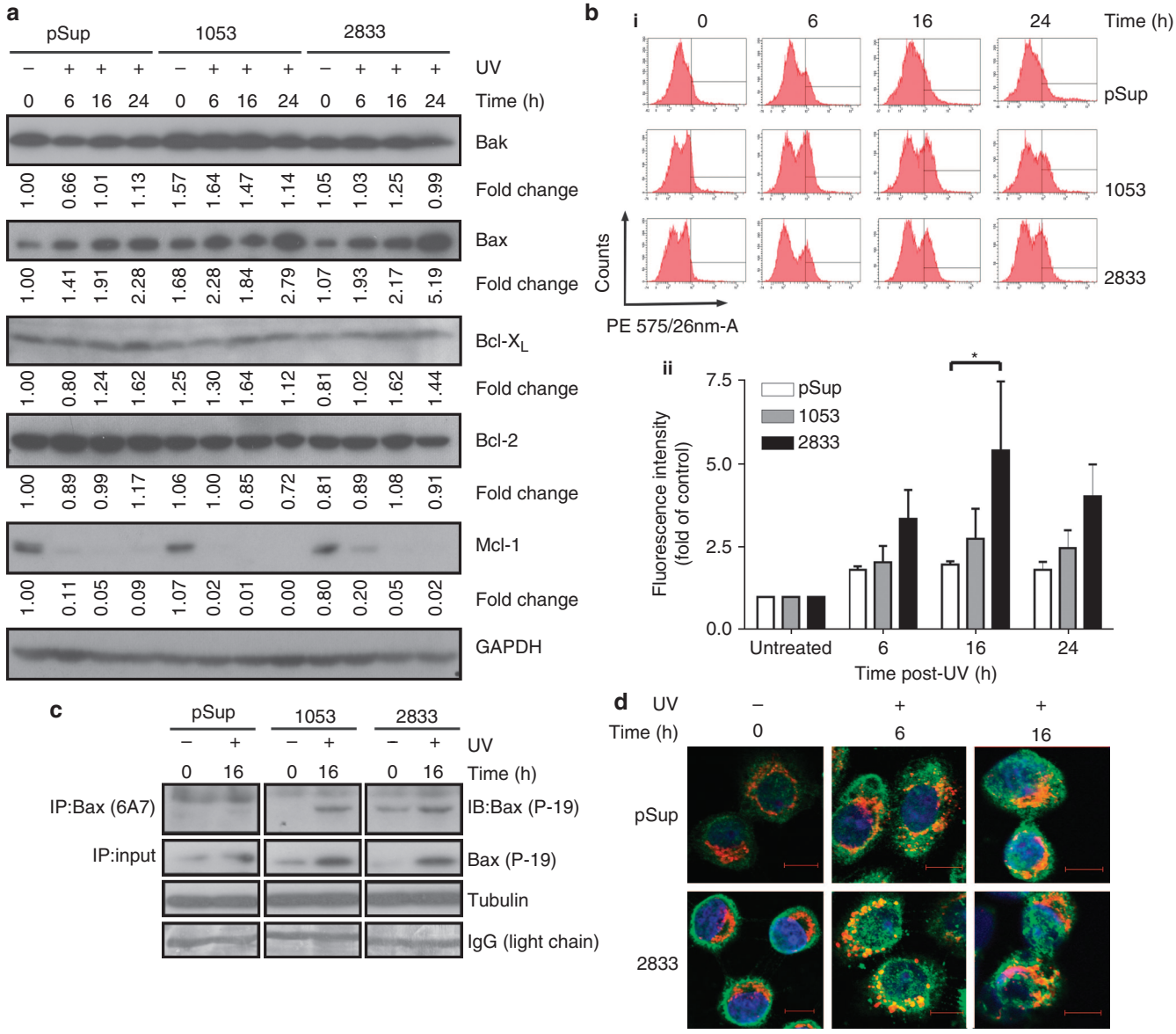

Figure 4. UV treatment results in increased activation of Bax and Bak in Axl knock-down MET1 cells. (**a**) MET1 pSup, 1053, and 2833 cells were exposed to UV (20 mJ cm^{-2}) and expression levels of Bak, Bax, Bcl-X_L, Bcl-2, and Mcl-1 were detected in total cell lysates by immunoblotting. (**b**) UV-induced activation of Bak was detected by harvesting and immunostaining MET1 cells with the conformation-specific anti-Bak Ab-1 antibody followed by FACS analysis. (i) Histograms from one experiment are shown; (ii) data (mean ± SEM) are expressed as fold of respective controls from two independent experiments. *$P<0.05$. (**c**) Active monomeric Bax was detected by immunoprecipitation using the monoclonal conformation-specific anti-Bax 6A7 antibody followed by immunoblotting with the polyclonal anti-Bax P-19 antibody. (**d**) Confocal microscopy was performed using the anti-Bax 6A7 antibody and the mitochondrial dye mitotracker orange. Bax (green) localization to the mitochondria (red) in response to UV is shown in yellow. Nuclei were counterstained with DAPI (blue). A representative image of the staining pattern is shown from three separate experiments. Bar = 10 μm.

SCC cells resulted in significantly greater caspase activity and apoptosis in response to UV compared with control cells. A previous study using a head and neck SCC cell line demonstrated that one of the most significant repercussions of deregulated Akt signaling is disruption of the apoptotic response to UVB (Decraene *et al.*, 2004). Knock-down of Axl did not majorly affect total or phosphorylated basal levels of Akt. However, Axl knock-down resulted in a pronounced loss of UV-induced Akt phosphorylation and was accompanied by dephosphorylation of the BH3-only protein Bad, which is known to enhance the ability of Bad to antagonize Bcl-2 and Bcl-X_L anti-apoptotic activities (Zha *et al.*, 1996; Datta *et al.*, 1997). Our findings are consistent with previous studies showing that Axl functions via Akt to enhance cell survival (Goruppi *et al.*, 1999; Lee *et al.*, 2002; Sawabu *et al.*, 2007).

To further clarify the mechanism of Akt dephosphorlation, we focused on PTEN, a known antagonist of Akt-dependent cell survival (Stambolic *et al.*, 1998). Axl has previously been shown to interact with C1-TEN, a PTEN homolog (Hafizi *et al.*, 2002); however, no association has

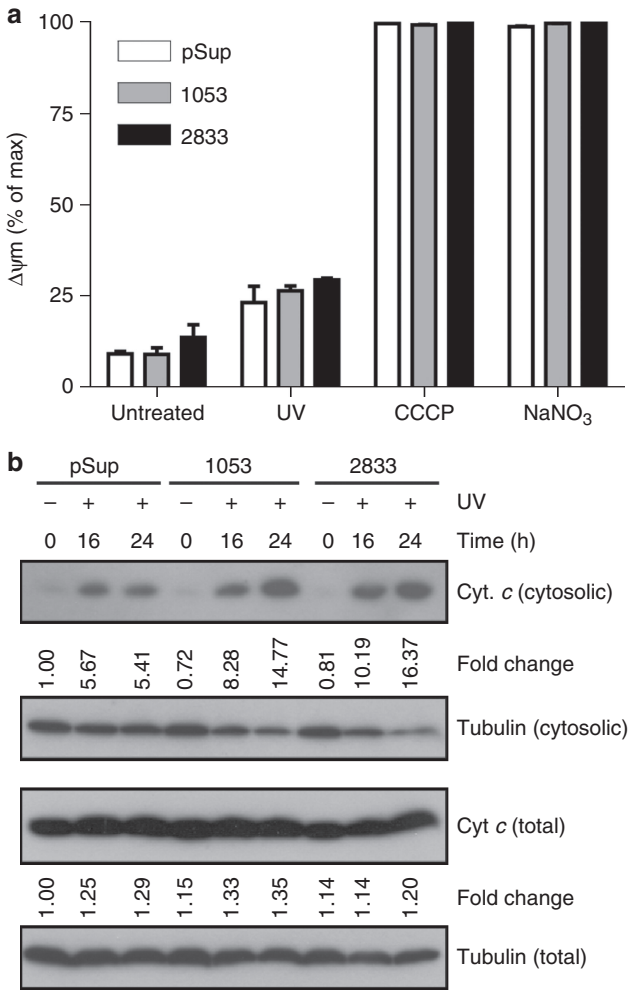

Figure 5. Increased UV-induced cytochrome *c* release in Axl knock-down cells. (**a**) Cells were harvested after 16 hours of UV treatment (20 mJ cm^{-2}). Treatment with carbonyl cyanide 3-chlorophenylhydrazone (CCCP) or $NaNO_3$ for 2 hours was used as a positive control for mitochondrial depolarization. A change in mitochondrial membrane potential ($\Delta\psi m$) was assessed by tetramethylrhodamine ethyl ester perchlorate and DAPI staining followed by FACS analysis. Data (mean ± SEM) are expressed as percent of maximum of respective controls. (**b**) Cytochrome *c* was detected in digitonin-extracted cytosolic fractions and in total cell lysates by immunoblotting. Data are representative of three independent experiments.

been reported between Axl and PTEN. Interestingly, our results revealed that knock-down of Axl markedly increased basal PTEN phosphorylation and led to a decrease in total PTEN levels in response to UV treatment. Recent studies have reported that the activity of PTEN is related to its phosphorylation status at the C-terminal ''tail'', with dephosphorylation resulting in decreased protein stability with a coincident increase in activity (Vazquez *et al.*, 2000, 2001). The increased phosphorylation of PTEN in the Axl knock-down cells could explain the loss of Akt phosphorylation in response to UV treatment, positioning Axl as a negative regulator of PTEN activity.

We next investigated the effect of knocking down Axl on the activities of Bax and Bak, two proteins that are required for commitment to cell death (Wei *et al.*, 2001). A change in the conformation of Bax and Bak was detected within 6 hours of UV treatment. This was accompanied by cytochrome *c* release, which was greater in Axl knock-down cells. This would imply that cytochrome *c* release takes place in a regulated manner through the formation of specific channels involving Bax and Bak and is negatively regulated by Axl.

Examination of anti-apoptotic proteins revealed that consistent with previous studies (Nijhawan *et al.*, 2003), Mcl-1 was equally down-regulated in response to UV in pSup and Axl knock-down cells. Contrary to a previous report (Qin *et al.*, 2006), UV treatment did not alter expression levels of Bcl-2 and Bcl-X_L in MET1 cells. In an attempt to characterize further the mechanism by which Axl modulates apoptosis, the expression of Bid, a crucial protein in the crosstalk between receptor- and mitochondria-mediated pathways, was examined. Basal expression of Bid was reduced in Axl knock-down cells, suggesting that Axl may have a role in regulating Bid stability. Bid cleavage became evident after cytochrome *c* release had been detected and was proportional to the degree of Axl knock-down. Additionally, inhibition of caspases blocked cleavage of Bid, but did not affect cytochrome *c* release into the cytosol, indicating it is unlikely for this process to have been driven by Bid cleavage. Thus, cleavage of Bid likely occurs downstream of Bax and Bak activation and is catalyzed by caspases. Contrary to previous studies, which have described Bid cleavage as an amplification step to the apoptotic process downstream of cytochrome *c* release (Slee *et al.*, 2000), our data using siRNA to target Bid expression reveal a redundant role for Bid in UV-induced cell death in accordance with previous studies (Kaufmann *et al.*, 2007). Our data suggest that SCC cells die predominantly via the mitochondria-mediated pathway.

In summary, our data demonstrate that Axl controls the relative balance between Akt and PTEN activities to modulate the apoptotic response in cutaneous SCC through negative regulation of Bak and Bak and to a lesser extent the BH3-only protein Bad, providing a mechanism for the role of Axl in cutaneous SCC resistance to apoptosis. Because Axl is located at the cell membrane, successful inhibition of its activity will potentially decrease downstream intracellular signaling and impede tumor development without the risk associated with intracellular feedback loops. The value of Axl as a therapeutic target has been validated using potent Axl kinase inhibitors that inhibited breast cancer cell motility and invasion (Zhang *et al.*, 2008). More recently, R428, a selective small-molecule inhibitor of Axl, has been demonstrated to prolong survival in animal models of metastatic breast cancer (Holland *et al.*, 2010). Our data support a role for Axl as a target for therapeutic intervention in cutaneous SCC.

MATERIALS AND METHODS

Cell culture and treatments

Spontaneously immortalized SCC cells (MET1 and SCC-IC1) (Proby *et al.*, 2000; Martins *et al.*, 2009) were cultured as described previously (Rheinwald, 1980). The pan-caspase inhibitor zVAD-fmk (Promega, Southampton, Hampshire, UK) or the Akt inhibitor SH5 (Enzo Life Sciences, Exeter, UK) was added to the media 1 hour before UV stimulation and during treatment.

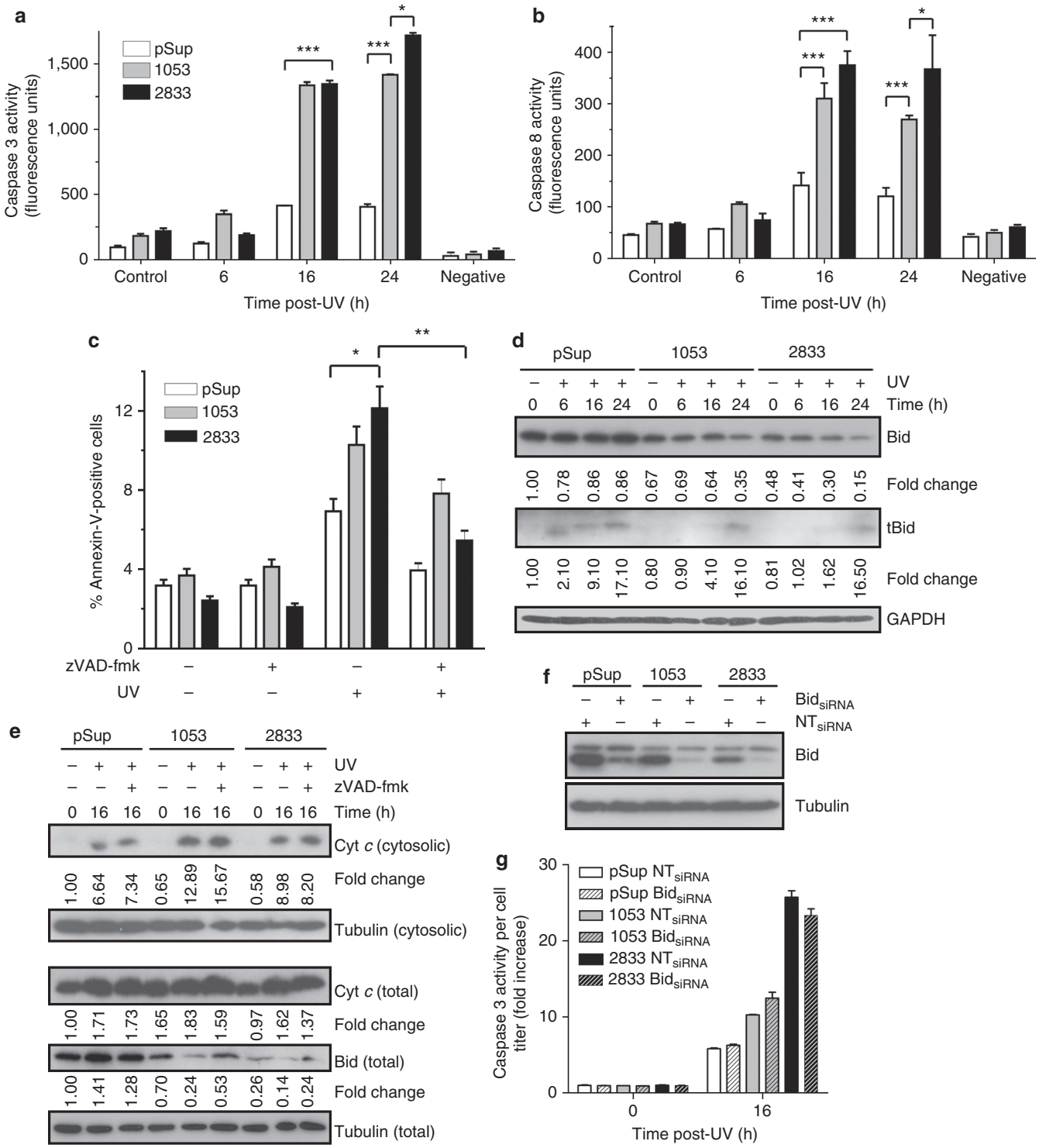

Figure 6. Axl knock-down diminishes expression of Bid, a protein that has a redundant role in caspase-dependent cell death. MET1 pSup, 1053, and 2833 cells were treated with UV for the indicated times in the presence or absence of zVAD-fmk (25 μM), and activities of (**a**) caspase 3 and (**b**) caspase 8 were quantified by incubating total cell lysates with specific fluorogenic substrates. (**c**) Apoptosis was quantified by Annexin V-FITC/PI staining of pSup, 1053, and 2833 cells treated or not with UV (20 mJ cm^{-2}) and/or zVAD-fmk for 16 hours. Data (mean ± SEM) shown are from three independent experiments. *$P<0.05$, **$P<0.01$. (**d**) Cells were harvested after UV treatment and expression levels of full-length Bid and tBid were detected in total cell lysates by immunoblotting. (**e**) Cells were pre-incubated with zVAD-fmk and were subsequently treated with UV for the indicated times. Cytosolic and total cytochrome *c* and total Bid levels were examined by immunoblotting. (**f**) pSup, 1053, and 2833 MET1 cells were transiently transfected with Bid or non-targeting (NT) siRNA (50 nM) and immunoblot analysis for Bid was carried out 96 hours post-transfection. Tubulin was used as a loading control. (**g**) Bid_{siRNA}- or NT_{siRNA}-transfected MET1 cells were treated with UV for 16 hours and apoptosis was determined by calculating the ratio of caspase 3 activity over cellular ATP content (cell titer). Data (mean ± SEM) are expressed as fold change of respective controls.

RNA interference, retroviral generation and delivery

Oligonucleotides corresponding to different target sequences were generated using OligoEngine RNAi Design Tool (Ambion, Huntingdon, UK). shRNA target sequences are listed below with their starting positions in the coding region of Axl: (1053) 5′-GACATCCTC TTTCTCCTGC-3′ and (2833) 5′-GATTTGGAGAACACACTGA-3′. Annealed oligonucleotides were cloned into pSup linearized by *Bgl*II and *Hin*dIII downstream of the H1 promoter TATA box. pSup or shRNA-containing plasmids were transfected into Phoenix packaging cells (Orbigen, San Diego, CA) using FuGene 6 (Roche, Welwyn Garden City, UK). At 2 days post transfection, cells were incubated in DMEM supplemented with 10% fetal bovine serum, 2 mM L-glutamine, and 1.25 μg ml^{-1} puromycin. Puromycin-resistant cells were maintained in selection media and were subcultured when 80% confluent. Confluent cells were placed in a humidified incubator at 32 °C for 12 hours to produce retrovirus-containing supernatant, which was used to infect SCC cells as described (Akgul *et al.*, 2005). Transient cell transfections of non-targeting or Bid ON-TARGETplus SMARTpool siRNA (50 nM) sequences were performed using Dharmafect as described previously (Martins *et al.*, 2009).

UVB irradiation

The UVB source was a UVP Multiple Ray Lamp (Ultra-violet Products, Cambridge, UK) (MRL-58 model) with emission at 302 nm, which was calibrated before each experiment. Cells were then replenished with fresh media.

Cell extracts and immunoblotting

Cells were lysed in Triton lysis buffer (TLB) as described previously (Tournier *et al.*, 2000). Cytosolic extracts were prepared using mannitol buffer with digitonin (80 μg ml^{-1}) as described (Lee *et al.*, 2006) and were concentrated using Microcon Bioseparations centrifugal filters (Millipore, Watford, UK). Protein content was normalized using a Bio-Rad DC assay. Following SDS-PAGE, proteins were transferred onto a Hybond-P membrane (Bio-Rad Laboratories, Hemel Hempstead, UK) using wet transfer. Membranes were saturated in Tris-buffered saline, pH 7.6, with 0.1% Tween 20 (Sigma-Aldrich Company, Dorset, UK) and 5% non-fat-dried milk (Marvel, Premier Foods, St Albans, UK). Antibodies against Akt, P-Akt Ser^{473}, AIF, Bad, caspase 3, PARP, Bcl-2, and Mcl-1 from Cell Signalling Technology (Danvers, MA), Bcl-X_L (H-62), Bax (P-19), Axl (C-20), phospho-PTEN (P-PTEN) Ser^{380} and P-Bad Ser^{136} from Santa Cruz Biotechnology (Santa Cruz, CA), PTEN from Millipore, Bid from R&D Systems (Minneapolis, MN), cytochrome *c* from BD Biosciences (Oxford, UK), Bak (Ab-1), tubulin from EMD Chemicals (Gibbstown, NJ) and GAPDH from Abcam (Cambridge, UK) were used for immunodetection. Secondary antibodies coupled to horseradish peroxidase were from Dako. Signals were detected by ECL + (GE Healthcare Life Sciences, Buckinghamshire, UK). Densitometry was performed by ImageJ 1.41 and values were normalized to total protein and expressed as fold change.

FACS analysis

Apoptosis was detected using TACS Annexin V-FITC (R&D Systems). Mitochondrial membrane depolarization was assessed by uptake of TMRE (Invitrogen, Paisley, UK). Carbonyl cyanide 3-chlorophenylhydrazone (CCCP, 100 μM) and $NaNO_3$ (1% v/v) were used as positive controls. TMRE (40 nM) was added to the media 30 minutes before the end of treatment and cells were trypsinized and washed with PBS. Cell pellets were resuspended in HEPES (250 μM) and DAPI (50 ng ml^{-1}) was added 10 minutes before FACS analysis. To assess activation of Bak, cells were fixed with PBS/0.25% paraformaldehyde, harvested by scraping and permeabilized with PBS/0.01% saponin. Cells were incubated with anti-Bak Ab-1 mouse monoclonal antibody (1/50 dilution) and then phycoerythrin-conjugated (Dako, 500 mg l^{-1}; 1/30 dilution) antibody while mixing (4 °C, 30 minutes). Mouse IgG was used as a negative control. Analysis was performed with a Becton Dickinson LSRII flow cytometer (BD Biosciences) using BD FACSDiva 6.0 software.

Caspase, viability, and proliferation assays

Activities of caspases 3 and 8 were measured fluorometrically using Ac-DMQD-AMC or Ac-LETD-AFC substrates (Enzo Life Sciences) following the manufacturer's instructions. Substrate cleavage was assessed by monitoring fluorescence intensity. Cell viability and caspase 3 activity of cells grown in 96-well plates (30,000 cells per well) were measured using CellTitre-Glo and Caspase-Glo 3/7 Luminescent assays (Promega), respectively, according to the manufacturer's instructions. The intensity of fluorescence and luminescence was measured using a Synergy 4 Multi-Mode Microplate Reader. The ratio of caspase 3/7 activity over cellular ATP content (cell titer) was used as a measure of apoptosis. Cell proliferation was determined by trypsinizing and counting cells exhibiting trypan blue dye exclusion.

Immunoprecipitation

Protein A agarose Fast Flow beads (Upstate) were mixed with 2 μg anti-Bax 6A7 antibody (Sigma) on a rotating wheel (4 °C, 2 hours). Antibody–bead complexes were washed thrice in TLB, combined with pre-cleared cell lysates, and immunoprecipitated on a rotating wheel (4 °C, overnight). Antigen–antibody complexes were washed four times in TLB and the reaction was stopped by adding 6 × Laemmli buffer and heating the samples (95 °C, 5 minutes).

Histology and immunostaining

Archival paraffin blocks were used with ethics approval obtained from the East London and City Health Authority Research Ethics Committee. Expression of Axl and P-Akt Ser^{473} was examined using immunohistochemistry on 4 μm deparaffinized sections blocked with horse serum. Immunostaining was performed as described previously (Jackson *et al.*, 2002). Apoptotic cells were detected in SCC sections by TUNEL assay (Dead-End, Promega). Quantitative analysis of staining was performed using KS400 version 3.0 imaging software (Carl Zeiss, Welwyn Garden City, UK). Staining intensity was scored by counting cells in four representative high-power fields, and was graded as 0 (no staining), 1 (weak), 2 (moderate), and 3 (intense). The anti-Bax 6A7 antibody was used to detect active monomeric Bax in cells. Mitochondria were stained with 100 nM mitotracker orange (Molecular Probes) for 30 minutes in a humidified atmosphere of 37 °C, 10% CO_2, and 90% air. Acetone: methanol (1:1)-fixed cells were blocked in PBS, 0.1% Triton X-100, 3% (w/v) bovine serum albumin, and incubated with primary (4 °C, overnight) and AlexaFluor 488-conjugated (Molecular Probes) secondary antibodies (room temperature, 1 hour). Nuclei were counterstained with DAPI (1 μg ml^{-1}) and samples were mounted onto glass slides using Immu-Mount (Thermo Fisher Scientific, Waltham, MA). Images were captured using a Zeiss LSM 510 META laser-scanning microscope.

Statistical analysis

Statistical significance was determined by one-way analysis of variance (ANOVA), with *post hoc* Tukey's test for comparison

between groups. Two-way ANOVA with Bonferroni correction for comparison between replicate means was used for time-course treatments.

CONFLICT OF INTEREST

The authors state no conflict of interest.

ACKNOWLEDGMENTS

This work was funded by the Association for International Cancer Research (03-0315), the British Skin Foundation, and Debra Ireland. We would like to acknowledge the generous gift of SCC cell lines from Irene Leigh and Charlotte Proby, Cancer Research UK Skin Tumour Laboratory, and Vera Martins for help with photography.

SUPPLEMENTARY MATERIAL

Supplementary material is linked to the online version of the paper at http://www.nature.com/jid

REFERENCES

Akgul B, Garcia-Escudero R, Ghali L *et al.* (2005) The E7 protein of cutaneous human papillomavirus type 8 causes invasion of human keratinocytes into the dermis in organotypic cultures of skin. *Cancer Res* 65:2216–23

Brantsch KD, Meisner C, Schonfisch B *et al.* (2008) Analysis of risk factors determining prognosis of cutaneous squamous-cell carcinoma: a prospective study. *Lancet Oncol* 9:713–20

Datta SR, Dudek H, Tao X *et al.* (1997) Akt phosphorylation of BAD couples survival signals to the cell-intrinsic death machinery. *Cell* 91:231–41

Decraene D, Van Laethem A, Agostinis P *et al.* (2004) AKT status controls susceptibility of malignant keratinocytes to the early-activated and UVB-induced apoptotic pathway. *J Invest Dermatol* 123:207–12

Diepgen TL, Mahler V (2002) The epidemiology of skin cancer. *Br J Dermatol* 146(Suppl 61):1–6

Erb P, Ji J, Wernli M *et al.* (2005) Role of apoptosis in basal cell and squamous cell carcinoma formation. *Immunol Lett* 100:68–72

Goruppi S, Ruaro E, Varnum B *et al.* (1999) Gas6-mediated survival in NIH3T3 cells activates stress signalling cascade and is independent of Ras. *Oncogene* 18:4224–36

Green J, Ikram M, Vyas J *et al.* (2006) Overexpression of the Axl tyrosine kinase receptor in cutaneous SCC-derived cell lines and tumours. *Br J Cancer* 94:1446–51

Hafizi S, Alindri F, Karlsson R *et al.* (2002) Interaction of Axl receptor tyrosine kinase with C1-TEN, a novel C1 domain-containing protein with homology to tensin. *Biochem Biophys Res Commun* 299:793–800

Holland SJ, Pan A, Franci C *et al.* (2010) R428, a selective small molecule inhibitor of Axl kinase, blocks tumor spread and prolongs survival in models of metastatic breast cancer. *Cancer Res* 70:1544–54

Jackson S, Ghali L, Harwood C *et al.* (2002) Reduced apoptotic levels in squamous but not basal cell carcinomas correlates with detection of cutaneous human papillomavirus. *Br J Cancer* 87:319–23

Kaufmann SH, Desnoyers S, Ottaviano Y *et al.* (1993) Specific proteolytic cleavage of poly(ADP-ribose) polymerase: an early marker of chemotherapy-induced apoptosis. *Cancer Res* 53:3976–85

Kaufmann T, Tai L, Ekert PG *et al.* (2007) The BH3-only protein bid is dispensable for DNA damage- and replicative stress-induced apoptosis or cell-cycle arrest. *Cell* 129:423–33

Kim H, Rafiuddin-Shah M, Tu HC *et al.* (2006) Hierarchical regulation of mitochondrion-dependent apoptosis by BCL-2 subfamilies. *Nat Cell Biol* 8:1348–58

Kluck RM, Bossy-Wetzel E, Green DR *et al.* (1997) The release of cytochrome c from mitochondria: a primary site for Bcl-2 regulation of apoptosis. *Science* 275:1132–6

Kuwana T, Newmeyer DD (2003) Bcl-2-family proteins and the role of mitochondria in apoptosis. *Curr Opin Cell Biol* 15:691–9

Lay JD, Hong CC, Huang JS *et al.* (2007) Sulfasalazine suppresses drug resistance and invasiveness of lung adenocarcinoma cells expressing AXL. *Cancer Res* 67:3878–87

Lee WK, Abouhamed M, Thevenod F (2006) Caspase-dependent and -independent pathways for cadmium-induced apoptosis in cultured kidney proximal tubule cells. *Am J Physiol Renal Physiol* 291:F823–32

Lee WP, Wen Y, Varnum B *et al.* (2002) Akt is required for Axl-Gas6 signaling to protect cells from E1A-mediated apoptosis. *Oncogene* 21:329–36

Letai A, Bassik MC, Walensky LD *et al.* (2002) Distinct BH3 domains either sensitize or activate mitochondrial apoptosis, serving as prototype cancer therapeutics. *Cancer Cell* 2:183–92

Luo X, Budihardjo I, Zou H *et al.* (1998) Bid, a Bcl2 interacting protein, mediates cytochrome c release from mitochondria in response to activation of cell surface death receptors. *Cell* 94:481–90

Martins VL, Vyas JJ, Chen M *et al.* (2009) Increased invasive behaviour in cutaneous squamous cell carcinoma with loss of basement-membrane type VII collagen. *J Cell Sci* 122:1788–99

Meric F, Lee WP, Sahin A *et al.* (2002) Expression profile of tyrosine kinases in breast cancer. *Clin Cancer Res* 8:361–7

Nijhawan D, Fang M, Traer E *et al.* (2003) Elimination of Mcl-1 is required for the initiation of apoptosis following ultraviolet irradiation. *Genes Dev* 17:1475–86

Proby CM, Purdie KJ, Sexton CJ *et al.* (2000) Spontaneous keratinocyte cell lines representing early and advanced stages of malignant transformation of the epidermis. *Exp Dermatol* 9:104–17

Qin JZ, Xin H, Sitailo LA *et al.* (2006) Enhanced killing of melanoma cells by simultaneously targeting Mcl-1 and NOXA. *Cancer Res* 66:9636–45

Rheinwald JG (1980) Serial cultivation of normal human epidermal keratinocytes. *Methods Cell Biol* 21A:229–54

Sainaghi PP, Castello L, Bergamasco L *et al.* (2005) Gas6 induces proliferation in prostate carcinoma cell lines expressing the Axl receptor. *J Cell Physiol* 204:36–44

Sawabu T, Seno H, Kawashima T *et al.* (2007) Growth arrest-specific gene 6 and Axl signaling enhances gastric cancer cell survival via Akt pathway. *Mol Carcinog* 46:155–64

Slee EA, Keogh SA, Martin SJ (2000) Cleavage of BID during cytotoxic drug and UV radiation-induced apoptosis occurs downstream of the point of Bcl-2 action and is catalysed by caspase-3: a potential feedback loop for amplification of apoptosis-associated mitochondrial cytochrome c release. *Cell Death Differ* 7:556–65

Stambolic V, Suzuki A, de la Pompa JL *et al.* (1998) Negative regulation of PKB/Akt-dependent cell survival by the tumor suppressor PTEN. *Cell* 95:29–39

Tournier C, Hess P, Yang DD *et al.* (2000) Requirement of JNK for stress-induced activation of the cytochrome c-mediated death pathway. *Science* 288:870–4

Vajkoczy P, Knyazev P, Kunkel A *et al.* (2006) Dominant-negative inhibition of the Axl receptor tyrosine kinase suppresses brain tumor cell growth and invasion and prolongs survival. *Proc Natl Acad Sci USA* 103:5799–804

Vazquez F, Grossman SR, Takahashi Y *et al.* (2001) Phosphorylation of the PTEN tail acts as an inhibitory switch by preventing its recruitment into a protein complex. *J Biol Chem* 276:48627–30

Vazquez F, Ramaswamy S, Nakamura N *et al.* (2000) Phosphorylation of the PTEN tail regulates protein stability and function. *Mol Cell Biol* 20:5010–8

Wei MC, Zong WX, Cheng EH *et al.* (2001) Proapoptotic BAX and BAK: a requisite gateway to mitochondrial dysfunction and death. *Science* 292:727–30

Zha J, Harada H, Yang E *et al.* (1996) Serine phosphorylation of death agonist BAD in response to survival factor results in binding to 14-3-3 not BCL-X(L). *Cell* 87:619–28

Zhang YX, Knyazev PG, Cheburkin YV *et al.* (2008) AXL is a potential target for therapeutic intervention in breast cancer progression. *Cancer Res* 68:1905–15